Energy and AI 14 (2023) 100287

Contents lists available at ScienceDirect

Energy and AI

journal homepage: www.elsevier.com/locate/egyai

RED WoLF hybrid energy storage system: Algorithm case study and green competition between storage heaters and heat pump

Alexander Alexandrovich Shukhobodskiy [a,*,1], Aleksandr Zaitcev [a,1], Giuseppe Colantuono [a,b,*,1]

[a] School of Built Environment, Engineering and Computing, Leeds Beckett University, Leeds, LS1 3HE, UK
[b] Watt Wolf Limited, 188-192 Commonside, Batley, England, WF17 6EB, UK

GRAPHICAL ABSTRACT

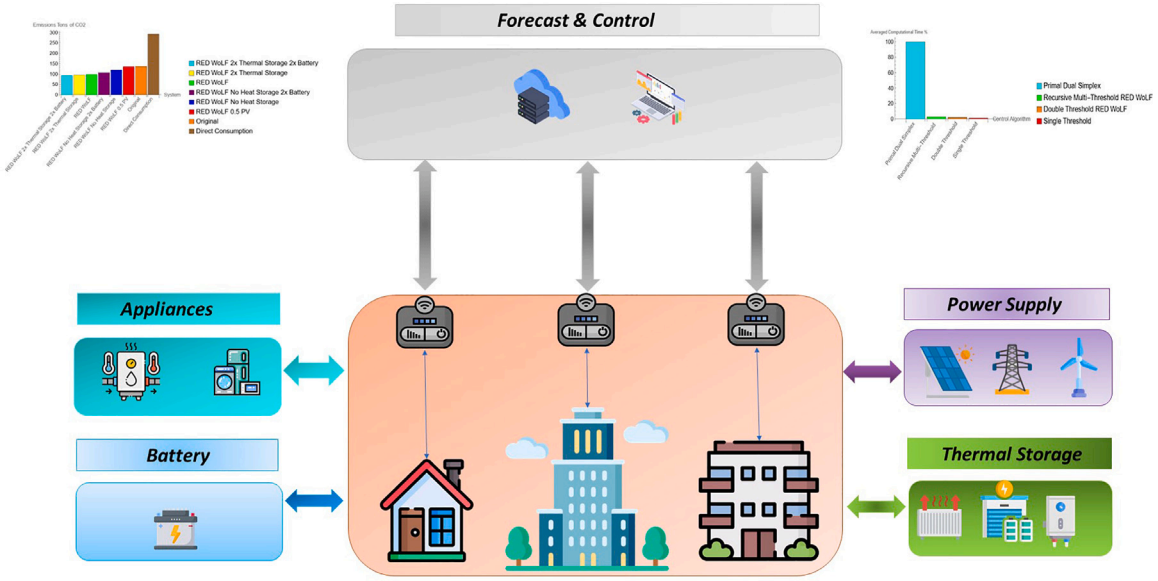

HIGHLIGHTS

- Controlling algorithm applicable to edge systems.
- Competition Between Storage Heaters and Heat Pump.
- Reduction of CO_2 Emissions.

ARTICLE INFO

Keywords:
Hybrid energy storage
Photovoltaic
Artificial intelligence

ABSTRACT

Green house gases reduction is critical in current climate emergency and was declared as major target by United Nations. This manuscript proposes the progressive adaptive recursive multi threshold control strategy for hybrid energy storage system that combines thermal storage reservoirs, heat pumps, storage heaters,

* Corresponding authors.
E-mail addresses: a.shukhobodskiy@leedsbeckett.ac.uk (A.A. Shukhobodskiy), g.colantuono@leedsbeckett.ac.uk (G. Colantuono).
[1] All authors contributed equally.

https://doi.org/10.1016/j.egyai.2023.100287
Received 11 April 2023; Received in revised form 15 June 2023; Accepted 26 June 2023
Available online 4 July 2023

Green house gases
Energy management

photovoltaic array and a battery. The newest control strategy is tested in numerical experiment against primal dual simplex optimisation method as benchmark and previous iterations of RED WoLF threshold approaches. The proposed algorithm allows improvement in reduction of CO_2 emissions by 9% comparatively to RED WoLF double threshold approach and by 26% comparatively to RED WoLF single threshold approach. Besides, the proposed technique is at least 100 times faster than linear optimisation, making the algorithm applicable to edge systems. The proposed method is later tested in numerical experiment on two measured datasets from Luxembourg school and office, equipped with batteries and ground source heat pumps. The system allows the reduction of CO_2 emission and improvement of self-consumption, size reduction of the photovoltaic array installed at the facilities by at least by half as well as substituting battery storage by thermal storage, reducing the initial investment to the system. Intriguingly, despite 3.6 times difference in efficiency between heat pumps and storage heaters, the system equipped with latter have potential to achieve similar performance in carbon reduction, suggesting that energy storage have more prominent carbon reduction effect, than the power consumption, making cheaper systems with storage heaters a possible alternative to heat pumps.

List of Acronyms

AI	Artificial Intelligence
BESS	Battery Energy Storage System
CCS	Carbon Capture and Sequestration
DHW	Domestic Hot Water
HP	Heat Pump
EU	European Union
GHG	Green House Gases
HSS	Hybrid Storage System
NWE	North West Europe
PV	Photovoltaic
RED WoLF	Rethink Electricity Distribution Without Load Following
SHs	Storage heaters
The Grid	Electric Grid
The UK	The United Kingdom of Great Britain and Northern Ireland

Variables

b	Back coefficient
T	Horizon period of Execution
t	Time of Execution

1. Introduction

Reduction of green house gases emissions was declared as major target on United Nations Climate Change Conference [1]. Moreover, decarbonisation is also one of the main aims of EU (European Union) [2]. Kotsopoulos [3] analysis suggested that energy conservation strategies and inventions are paramount for the society well being and overall sustainability. Smart energy usage is one of the main goals of EU innovation and cooperation programs such as [4,5]. The report from flo [6] suggested that approximately 30% or 41.1 million of tonnes of oil equivalent contribute to energy consumption in residential sector, whereas approximately 15% or 20.7 million of tonnes of oil equivalent was consumed by public buildings, offices and commercial facilities. As a result, targeting these sectors with smart energy systems being valuable in current conditions.

The price of energy varies throughout the day on the wholesale level as well for time-of-use-tariff or dynamic tariff [7]. Similarly CO_2 associated to generated energy unit possess variability [8,9]. Such phenomena are associated with different power generation sources and mismatch between cleaner and renewable energy sources and energy consumption demand. In case there is not enough power supply, less efficient fossil fuel power stations are started to satisfy the demand requirements, as other energy sources do not possess flexibility or are more restrictive. In order to tackle this mismatch energy storage may be used, to reduce the need of high emission single-cycle on-demand power plants.

One of the obstacles in energy storage penetration is the high initial cost. However, that could be reduced by separating energy storage reservoirs. Thus, adding required flexibility for the electrical grid (the Grid). Such solution is also relevant for futuristic renewable-only scenarios or in combination of thermal plants with carbon capture and sequestration (CSS) biofuel or both. In such cases the time of energy use is more significant than amount of power generation, making flexible energy storage reservoirs the necessary instrument in the prevention of renewables curtailment.

Significant amount of energy consumption is attributed to space heating in northern climates, whereas the demand for cooling is much lower. That makes batteries not being a cost effective solution due to their high cost per unit of energy capacity. Although, the cost of batteries is gradually reducing and thus could become of the comparable price, the life cycle and efficiency of contemporary batteries could contribute to energy loss due to additional energy conversion, making the separation between storage reservoirs for heating/cooling and other energy use still a preferable option. However, making the separation of storage reservoirs and power flows in a dynamic environment significantly increase computational complexity for systems that require to be controlled promptly. Thus requiring control strategies to be developed or adapted for the purpose, to achieve full benefit of hybrid energy storage systems.

1.1. State-of-the-art

There is a mismatch between the power consumption demand and renewable wind [10–12] or solar power generation, such as the “duck curve” [13,14]. Moreover, wholesale energy price could reach negative values [15]. The addition of energy storage system, appliance management or both have potential to reduce the effect of mismatch or completely negate it as well as exploit the negative energy pricing. The RED WoLF (Rethink Electricity Distribution Without Load Following) system combines thermal storage, electrochemical storage as well as renewable power generator in form of PV (Photovoltaic). These components are comprehensively analysed individually with HSS (hybrid energy storage systems) that combines multiple elements being the promising technological solution. The RED WoLF system is aimed to reduce CO_2 emission by storing energy from the grid to mitigate the mismatch as well as implicitly improve self-consumption of local renewable power generation. The relation between CO_2 emissions for various energy systems were investigated thoroughly by Wagh and Kulkarni [16]; Mohamad et al. [17]; Mohamad and Teh [18]; Grosspietsch et al. [19]. Thus, signifying the importance of energy management systems for green house gases reduction.

Since there is a mismatch between power generation by the PV array and power consumption addition of BESS [20,21], or appliances management [22] or both [23–26] have potential to improve self-consumption. The latter approach was strongly recommended by Uddin

et al. [27]. Reports of Sufyan et al. [28],Arani et al. [29] provide overview over BESS (battery energy storage systems) including BESS life-cycle and aging of batteries. Wu et al. [30] had focused on artificial intelligence (AI) applications to improve management BESS. Moreover, similar results could be achieved by controlling thermal energy storage [28,31]. More efficient technologies like HP (Heat Pump) require less energy to function with comparison to the direct heating. Nevertheless, both systems could produce heating on demand only with comparison to storage heaters (SHs) that could also store the energy. Consequently intake of more polluting energy might be taken from the electrical grid. Connecting thermal storage reservoirs to HP [32,33] provide the required flexibility. Reda and Fatima [34] considered the environmental aspect of HSS with combination of HP, SHs and a battery. Slightly different HSS with SHs, PV array, DHW (Domestic Hot Water) Cylinder and a Battery was considered by Shukhobodskiy and Colantuono [35]. Shukhobodskiy et al. [36] improved the [35] controlling technique and considered difference between following CO_2 signal and time of use tariff. Although all system performs relatively well in accordance to [37] it is difficult to achieve financial benefit by implementing BESS only.

The accuracy of consumption forecast traditionally assumed to be of importance for load flexibility in offices (e.g. [38]), residential dwellings (e.g. [39]) as well as educational facilities (e.g. [40]). Likewise, the precision of the generation forecast is significant for smart systems power consumption management in offices, residential dwellings and educational facilities (e.g. [41,42]). As a result, one of important aspects that is implemented in such systems is control strategy. Moreover, approaches such as reinforced learning could help operate energy systems equipped with batteries in microgrid (e.g. [43]). Implementing population models during the learning process have potential to improve the scheduling for the system as shown by Mounsif and Medard [44]. Though, [45] suggested implementing artificial intelligence to energy management systems could lead to additional cybersecurity risks that should taken into account and be mitigated. Furthermore, AI applications for renewable energy technologies are comprehensively discussed in [46,47].

Combinations of model predicted control and reactive control are widely employed in energy management systems. In case of model predictive control, the forecast of system behaviour should be employed. Some techniques such as dynamic thermal rating [48,49] have potential to improve quality of electricity intake. However, for dynamic systems composed of multiple elements computational complexity provide significant obstacle for white box (physics based models) to be implemented for multi-component systems favouring black box or hybrid approaches (combination of black and white boxes) for realistic applications with computational and temporal constrains (e.g. [42,50,51]). Such approach is in agreement with [52] that suggested to employ single threshold RED WoLF algorithm [35] for applications in edge devices in order to reduce the operational and initial costs for the HSS.

Moreover, [53] presented that adding the demand management to single threshold approach further improve the performance of the system, by adding negligible amount of computational time. Thus, improvement of fast paced algorithm provides interest for realistic applications. The computational simplicity of the RED WoLF model could be used to created hybrid neural network (physics informed neural network) and complement reinforced learning models. Furthermore, the approach employed for the RED WoLF system algorithm can be easily comprehended by bachelor and master level STEM (science, technology, engineering and mathematics) students, without previous experience in green energy technologies [54]. Thus, making RED WoLF threshold approach a potentially good educational introduction in understanding the Grid related CO_2 emissions and importance of energy management systems.

1.2. Novelty

The main contribution of this manuscript is introduction of the new fast control threshold based technique for hybrid energy storage systems and its application to residential, public buildings, offices and commercial facilities, that could accurately react to rapid changes of CO_2 emission forecast as well as power generation and power consumption predictions. Furthermore, the proposed RED WoLF system can now allow employment of HPs combined with battery or thermal storage (water tank, radiators), in contrast to most previous configurations that consider only SHs, DHW Cylinders, combined with battery storage and local PV array (e.g. [35]) or system only equipped with a HP accompanied by thermal storage and local PV array (e.g. [42]). [36] introduced progressive adaptive double threshold algorithm for the RED WoLF HSS [35]. Here a recursive progressive adaptive multi threshold algorithm is introduced and compared with primal dual simplex optimisation technique [55] and other RED WoLF controllers [35,36,56]. The results of numerical experiment are presented in this manuscript for both computational speed and performance comparison of algorithms for CO_2 reduction. Then the RED WoLF algorithm is tested in a case study for residential dwelling, an office and large school located in Luxembourg. The office and the school are equipped with battery storage and PV array as well as ground source HP. The grid consumption and CO_2 emissions of the RED WoLF controller is compared with measured data for various scenarios including the system equipped with more power consuming and much cheaper SHs, rather than more expensive heat pumps. Moreover, these comparisons are rare, since only few systems outside of RED WoLF HESS, employ combination of SHs, DHW Cylinder, Battery and PV array as well as considering reduction of CO_2 emissions being the ultimate goal of the system. As a result, this manuscript addresses three research gaps. The lack of novel development and implementation of threshold based controllers and potential ways of their evolution. The lack of intraday assessment of differences between CO_2 emissions reduction and associated electrical power grid reductions. The lack of HESS components comparison and CO_2 intensity forecast errors consideration for hybrid energy management systems.

2. System design and controlling algorithm

2.1. System design

The RED WoLF system benefits the environment by reducing the CO_2 emissions through improvement in the self-consumption and the Grid power consumption in the facility via smart controls. Previously the RED WoLF system was analysed in residential dwellings only (35, 36,52,56,57). In the present manuscript, the analysis is extended to for public buildings and offices and thus technologies such as HPs are incorporated to the control architecture of the RED WoLF system. The brief graphical description of the system is illustrated on Fig. 1. With the aid of local smart controller the RED WoLF is managing the power flow within the building. The devices could be separated into 5 different categories: the ones that can control (Smart Controller), the ones that can produce the power (Power Supply on Fig. 1), the ones that can store the energy (Energy Storage on Fig. 1), the ones that process the information (Data and Control on Fig. 1) and the ones the can only consume the power (Electrical Appliance on Fig. 1). Smart controller manages energy in several ways. First of all, it collects the information about the power consumption of devices involved in the RED WoLF information and sends in to the cloud server. In return smart controller receives sets of instructions for controllable elements of energy storage. In case the building equipped with HP connected to the thermal storage reservoirs then it is also being considered as a storage for DHW or space heating or both. The remote server is hosting the forecast service, where implementation of machine learning prediction models are implemented for the power consumption and generation, for each individual dwelling. On the same server the RED

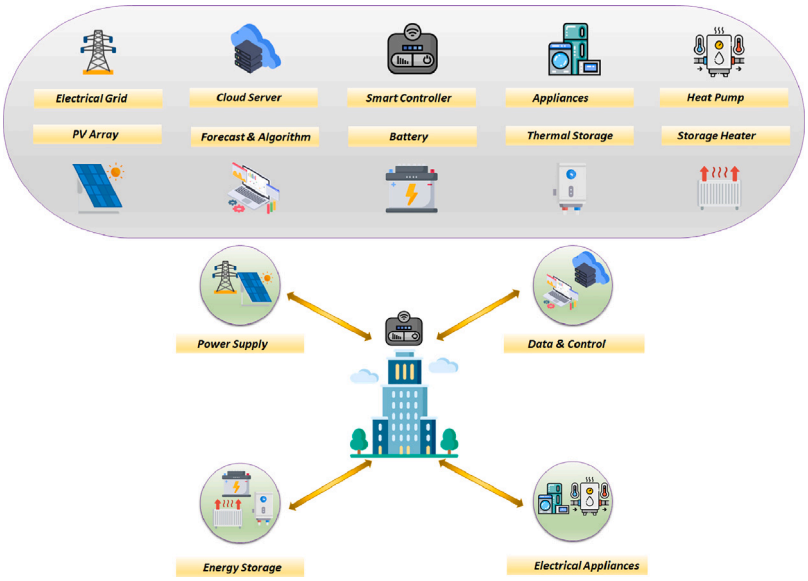

Fig. 1. RED WoLF main components.

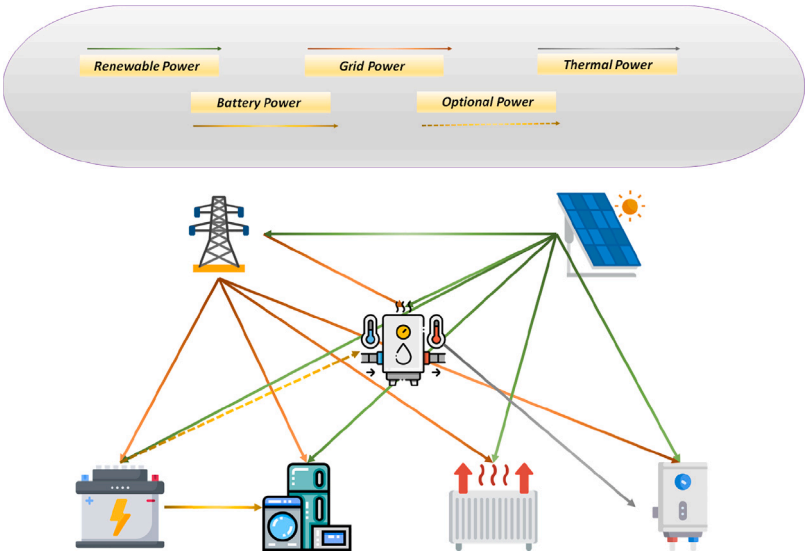

Fig. 2. RED WoLF Power Flow. Green arrows represent the energy flowing from the PV array, orange arrows represent the energy flow from the Grid, yellow line represents the energy flow from the Battery, dashed yellow line represents the optional energy flow from the battery to the HP or other space heating storage system and the grey line represents the thermal power flow from the HP to the thermal energy storage. All the icons depicted on this illustration are taken from [58]. (For interpretation of the references to colour in this figure legend, the reader is referred to the web version of this article.)

WoLF algorithm computes the necessary control commands for energy management systems.

In order to avoid stored energy waste, the battery is only allowed to be used on electrical appliances, so there is no double conversion between energy stored in electrochemical storage and thermal storage. This configuration is depicted in Fig. 2. The preferred energy source is the PV array, which is depicted as green arrows, and thus the power could be directed to all devices within the system. Similarly the Grid power is also allowed to be send to all devices. However, it is only used in the absence or insufficiency of renewable source and the use of stored energy would contribute to more CO_2 emissions or increase of price, whenever time-of-use-tariff is implemented. Indeed in some case in accordance to Octopus Energy Agile tariff [7] the retail Energy price could have negative values making the Grid preferable power source to local renewable power. There is also an optional ability to supply heating elements for thermal storage in a battery whenever it is more beneficial to reduce the GHG emissions or annual price, for systems with limited thermal storage. This could be the case if the system already has for example a HP and a battery of large capacity but lacks the thermal energy storage or its capacity is not sufficient. One example of such system could be ground sourced HP that distribute the energy through the series of pipes in a floor, in a ceiling, in walls or any combination of those. This system lacks the separate (discrete) thermal storage such as SHs. As a result such deviation allows additional functionality to the system by allowing battery usage for space heating application could be beneficial for GHG reduction. In this case the control strategy will treat HP as part of appliances for the required consumption needs for all the daily energy requirements that exceed the maximum capacity of thermal storage reservoirs. Although such strategy is not the most efficient one, it would allow to control existing systems without the need of retrofit, whereas newly constructed buildings should avoid such configuration.

The proposed [59] system is undergoing the testing phase in ≈ 100 residential dwellings across north-west Europe, in Ireland, France,

Luxembourg and the UK. With newly added Luxembourg pilots being equipped with ground source HPs and thermal storage instead of SHs.

2.2. Controlling algorithm

The foundation of the algorithm implemented for the control strategy is described in [36] and is briefly introduced in Appendix. Since then, significant improvements have been implemented to achieve better performance. The new approach is introduced in this manuscript and could be described similarly to the recursion process that modified the original RED WoLF control strategy [35] by Wiesheu et al. [56]. Though, the proposed recursion is now implemented for the adaptive double threshold approach presented in [36] and the recursion applied only to the main threshold. The schematic description of such modification is depicted on Fig. 3

Here the description starts from the middle panel on Fig. 3 that corresponds to the algorithm described in [36], however instead of original 24 hours horizon 48 hours horizon is implemented. This horizon is updated every 24 hours. The numbered yellow boxes correspond to important steps within the algorithm. In the panel before step one there is CO_2 intensity index forecast for 48 hours period at time T_n which is then updated into new 48 hours forecast horizon at $T_n + 24$. In between these steps the new forecast for CO_2 intensity is updated hourly, within the current horizon interval. Furthermore, during 24 hours period starting from time T_n the horizon is unchanged unless it reaches the value $T_n + 24$, where T_0 is initial starting time of the system. Thus, the connection between T_{n+1} and T_n is given by

$$T_{n+1} = T_n + 24 \text{ h}. \tag{1}$$

At time T_n the targets for energy storage are set and forecast. These targets must be satisfied by the end of 48 hours horizon period. These targets are updated at least at 24 hours period which is novel to the process and would insure the smoothness of operation. Though, the resolution could be arbitrary but not less than threshold calculation resolution. Then at step one the CO_2 intensity index is sorted in increasing order to allow two thresholds: main threshold and auxiliary threshold being calculated by the method described [36] and briefly in Appendix. This allows to select time intervals for which the storage reservoirs would be charged and battery would be used. These periods are coloured in green and yellow colours respectively on Fig. 3. The green area is corresponding to the minimum amount of time for the grid electricity being directed to the dwelling. This time is calculated by estimating the difference between forecast of energy consumption and forecast of energy generation within the dwelling divided by maximum possible power intake from the Grid. Every value of sorted CO_2 intensity correspond to specific time. By selecting the lowest execution region of CO_2 intensity index, the process also allows to obtain corresponding temporal values. Then this time intervals are distributed across the original non-sorted CO_2 values by matching the time with corresponding CO_2 intensity levels. The process is similar for the yellow region and corresponds to time of battery discharge. However, selection is done for the sorting CO_2 intensity index at period of high levels of CO_2 intensity. Once this procedure is done we know the approximate minimum time of grid use as well as approximate time required for battery to be discharged. At step 2 we apply these areas to original CO_2 intensity forecast and implement the control commands of the algorithm on 1 minute resolution for one hour. Then, at step 3 the CO_2 intensity forecast the execution is employed for t hours, $1 < t \leq 24$. Thus, removing initial t hours from the CO_2 intensity forecast and execution. Afterwards we repeat sorting procedure 1, however on the shorter time interval and in step 5 execution of such process begins. This cycle is of steps 3 to 5 is repeated until t reaches value of 24 hours, afterwards in step 6 the new horizon is picked, here depicted as orange area. Important step to note is that after every hour of the execution the new forecast of CO_2 intensity is generated, dwelling consumption is metered and charge levels of storage reservoirs are measured/estimated and new thresholds are calculated to satisfy the initial or modified storage target. This process makes the threshold adaptive to intraday changes. Once the new horizon is selected, the whole procedure repeats.

Now the most significant novelty is the recursive correction to threshold calculations. Instead of executing the RED WoLF algorithm directly. The first step is to emulate the performance of the system in order to try to avoid direct use of electricity for DHW consumption and space heating. This procedure is depicted on the bottom panel at Fig. 3 under the box “Threshold Recursive”. All steps repeat the process of previous threshold calculation, however the new process is added. In case during the simulation phase there was a period of the direct space heating or domestic hot water usage during the execution (depicted as burgundy area in step 2), then modification to the forecast horizon is made and the back coefficient, b, is calculated. The back coefficient, b is the novel addition to the threshold calculation and is aimed to compute how many additional time periods are required to be added to the system schedule, so that the charging on demand is not forecast. Initially the coefficient for the 48 hours horizon is set up to be 0. Nevertheless, every time during 24 hours execution period back coefficient increases its value by 1 hour, whenever the event of direct usage of space and DHW occurs during the simulation. Moreover, once such event occurs whole simulation returns to the first procedure in the cycle, that determines the horizon forecast. However, now there is an updated back coefficient. The back coefficient works in a way similarly to the adaptive threshold update through time, however instead of removing initial hours from the forecast horizon for main threshold it adds b hours of extra storage time for the main threshold. In more details it insures that the areas corresponding to low CO_2 emissions are exploited (depicted as red area at step 3), rather than the burgundy area in previous step. Thus, increasing the amount of time for storage reservoirs to be charged at step 4 and then at step 5 new thresholds and execution periods are received. This procedure repeats until b reaches the value of 47 hours, or no events of direct heat usage occurred during simulation phase. As a result, the correction to threshold calculation is aimed to further reduce CO_2 emissions, by improving control over power intake in periods of low CO_2 intensity levels. Similar correction was introduced in [56] for the Original RED WoLF algorithm described in [35], though have not improved the algorithm performance significantly.

2.3. Comparison of controlling algorithms

In this subsection there is a comparison between RED WoLF Original Algorithm [35], RED WoLF Double Threshold Algorithm [36], RED WoLF Multi Threshold Recursive Algorithm introduced in this manuscript and Primal Dual Simplex Method ([55,60]). The latter is considered to be the case which is close to ideal global optimum solution. In order to proceed with Primal Dual Simplex Method, the pre-processing procedure [61] is employed to remove constrains and redundancies.

For this comparison the available annual CO_2 intensity data for the UK [8] at 2019 is employed. The PV generation profile from [62] and the power consumption profile from [63]. These datasets were previously employed in [36,64]. Moreover, the [63] data were detrended from any seasonal dependencies and scaled to average UK data [65] of 5 MWh. Moreover, the assumption is that the heating period starts in October and finishes at March with peak of 80 kWh day in January to 0 kWh in March. The DHW Cylinder of 10.5 kWh capacity and is assumed to be used from 7:00–7:50 in the morning and 17:30–18:20 in the evening. That is the period when the energy is drained from this storage reservoir. Furthermore, the battery capacity to be is chosen to be between 0–10 kWh. The PV array peak power varies from 0 to 10 kWh. It is also assumed the power supply is average for the UK household with maximum power intake from the Grid of 25 kW. As a

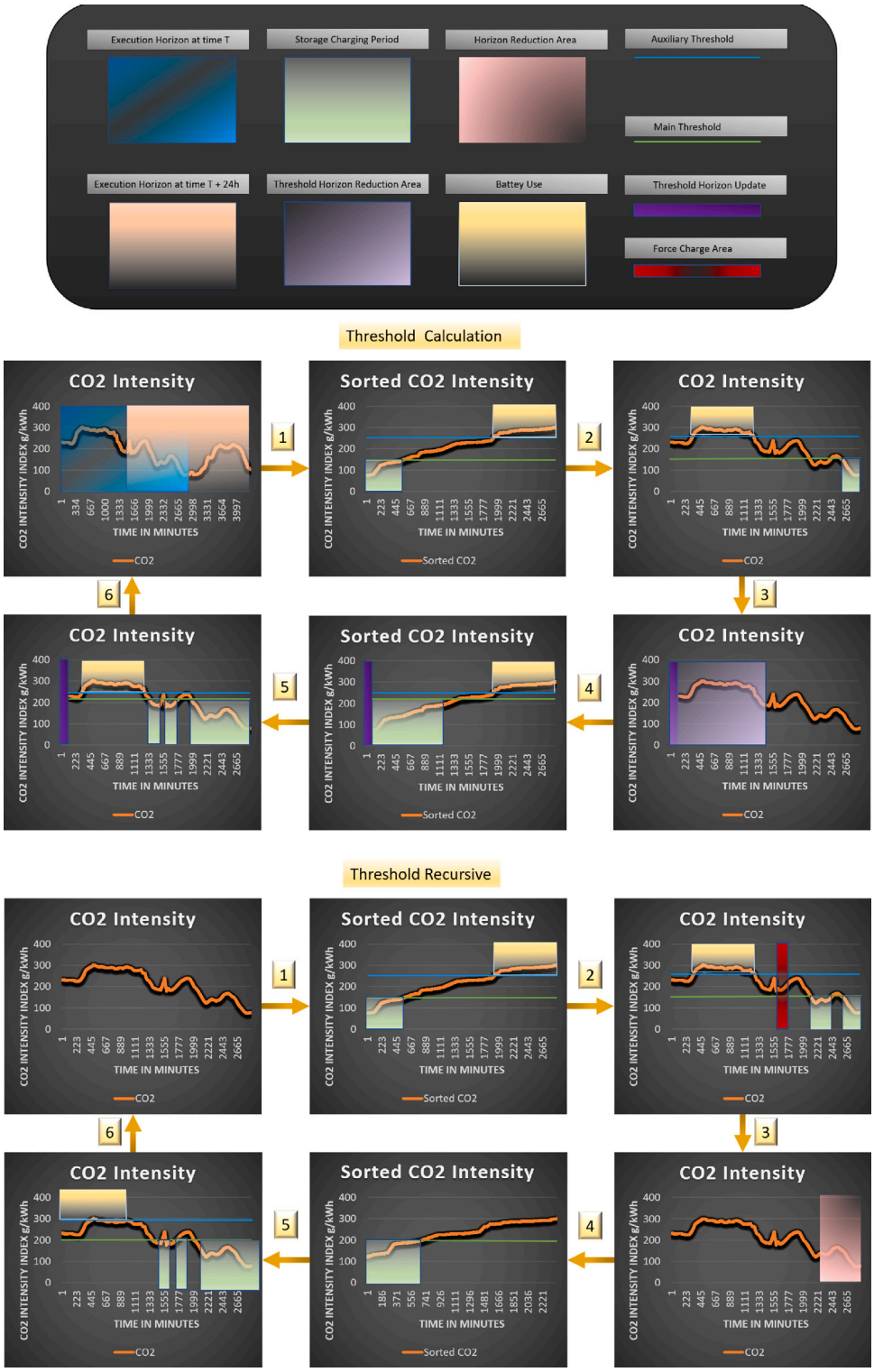

Fig. 3. Threshold Calculation Diagram. The top panel corresponds to the legends. The middle panel corresponds to standard calculation. The bottom panel corresponds to recursive update. Numbered yellow boxes correspond to significant steps in the algorithm. Shaded areas in steps 1 and 4 represent sections of Grid power intake on chronologically sorted CO_2 values. Shaded areas in step 2 map main threshold regions and auxiliary threshold regions from intensity-sorted CO_2 values back to chronologically-sorted CO_2 values. Shaded areas in steps 3 on middle and bottom processes represent time progression and thresholds correction respectively. Shaded areas in step 5 represents planned execution of the algorithm and map main threshold regions and auxiliary threshold regions from intensity-sorted CO_2 values back to chronologically-sorted CO_2 values. Step 6 represents forecast update. (For interpretation of the references to colour in this figure legend, the reader is referred to the web version of this article.)

result it is possible to compare the controlling techniques. The Primal Dual Simplex algorithm is used as benchmark to compare performance and in contrast to RED WoLF controller is made in 1 h resolution steps, rather than 1 min step. All numerical calculations are made on Python 3.6 Spider GUI 5.1.5, AMD Ryzen 7 5800H, Radeon Graphics 3.20 GHz, on Windows 11 OS. Results are presented on Fig. 4.

Primal Dual Simplex method still demonstrates the best accuracy. Since the average saving with Primal Dual Simplex algorithm are ≈ 69%

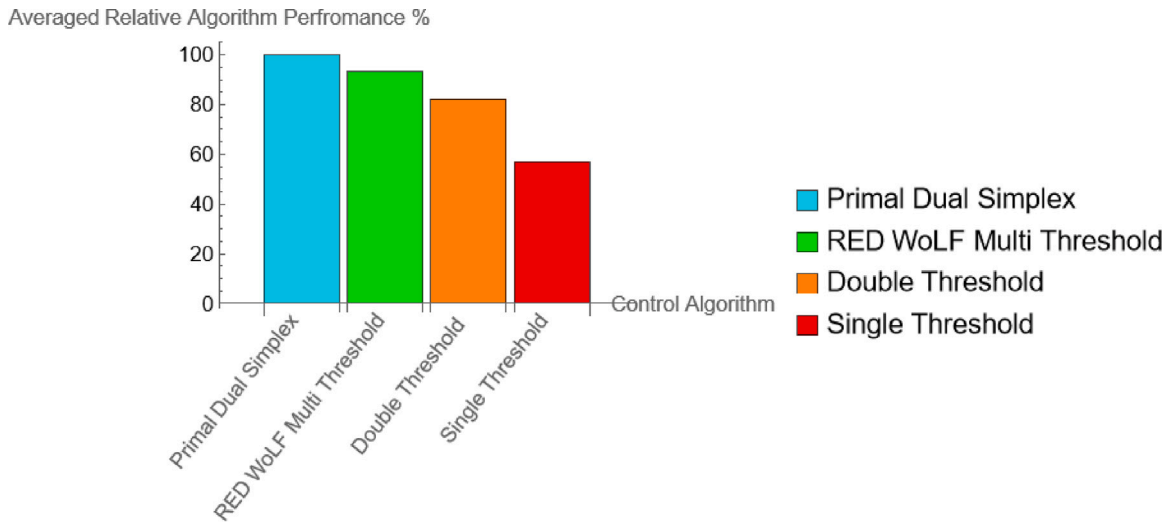

Fig. 4. Performance improvement comparison graph. The Blue box represent the Primal Dual Simplex, The green box represents Recursive Multi-Threshold RED WoLF Control Algorithm, the orange box represents Double Threshold RED WoLF Control Algorithm and the red box represents the original single threshold RED WoLF algorithm. (For interpretation of the references to colour in this figure legend, the reader is referred to the web version of this article.)

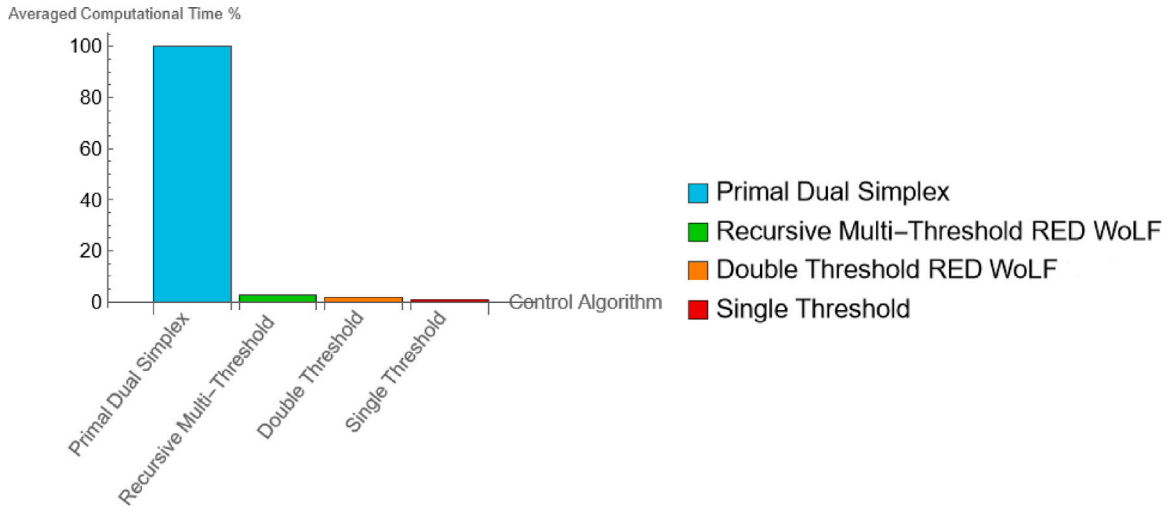

Fig. 5. Computational time controller performance comparison graph. The Blue box represent the Primal Dual Simplex, the green box represents Recursive Multi-Threshold RED WoLF Control Algorithm, the orange box represents Double Threshold RED WoLF Control Algorithm and the red box represents original single threshold RED WoLF algorithm. (For interpretation of the references to colour in this figure legend, the reader is referred to the web version of this article.)

that would make RED WoLF Multi Threshold approach suboptimal only by $\approx$ 4%. This difference is smaller than errors for CO_2 intensity and power consumption forecasts and thus might be neglected. For example root mean square percentage error for CO_2 is $\approx$ 24% in 2018, $\approx$ 73% in 2019, $\approx$ 8.6% in 2020, $\approx$ 7.5% in 2021 and $\approx$ 7.5% in 2022, in the UK in accordance to [8] data. Thus, the aggregate error for forecast would be even higher. Besides, the algorithms are much faster, with Primal Dual Simplex performance speed for one minute resolution being estimated to be over $\approx$ 3000 minutes, whereas the average speed of RED WoLF Multi-Threshold approach could vary between $\approx$ 10 and $\approx$ 30 minutes for annual simulations and take seconds for one day. These allow RED WoLF HSS to be implemented on and benefit from edge systems, or in case of more powerful computational device be part of more complex demand response system. Similar conclusion was made in [52] for the original RED WoLF HSS controller. Still, the RED WoLF algorithm was not optimised for faster performance and thus the execution speed might increase once this target would be set. The current comparison of computational speed of algorithm performance is presented on Fig. 5.

It is noted that, although there was slight speed increase due to introduction of additional thresholds and the recursion process this increase is still negligible, with comparison to the Primal Dual Simplex Method. Moreover, [52] demonstrated that the original RED WoLF Single Threshold Approach is significantly faster than [66] technique with speeds of $\approx$ 1 ms vs over $\approx$ 20 minutes computational time and had less charge and discharge cycles with $\approx$ 2–$\approx$ 3 less operational cycles implemented. The controller introduced in this manuscript has $\approx$ 329 of charge/discharge cycles during the year, whereas Single Threshold method has $\approx$ 238 of charge/discharge cycles and Primal Dual Simplex Method, has $\approx$ 394 charge/discharge cycles. We should note that neither of algorithms are aimed to minimise the rate of charge and discharge, and such phenomena occurs most likely naturally due to sinusoidal profile of grid CO_2 intensity index. By setting up a target of battery use throughout the day, the algorithm implicitly controls the charge/discharge cycle.

Moreover, since the algorithm operates with forecast values of consumption for appliances, domestic hot water, space heating and carbon intensity index. The accuracy of execution would be dependent on the accuracy of prediction. However, the effect of prediction with significant errors is mild for the RED WoLF algorithm, as is was designed with assumption that it is difficult to achieve precise predictions in open

Table 1
Annual CO_2 emission in tons in the office and in the school. Top row, corresponds to CO_2 emissions in the school. Bottom row corresponds to CO_2 emissions in the office. The left column corresponds to the RED WoLF system equipped. The middle column corresponds to emissions of the system without battery storage and PV array. The right columns corresponds to emissions of corresponding to measured values.

RED WoLF	Direct consumption	Original
343.9 t	292.5 t	135.8 t
9.7 t	11.3 t	8.1 t

dynamic systems, and thus must adapt promptly to constant changes in environment. Making the method prominent even for cases, where there is not enough data to create sophisticated predictions of power consumption and generation. The downside is that the result might be suboptimal for highly accurate predictions, and thus the RED WoLF algorithm might perform worse if there are only a few components to operate and change in the environment is less dramatic.

3. Case study: Application of RED WoLF in public buildings and offices

In this section the performance of the RED WoLF system is analysed for an small office and public school in Luxembourg area. The data for the numerical experiment was obtained from two Luxembourg companies [67,68]. The data analysed and employed in numerical experiment is from the school that has gross floor area of 46,000 m^2 with energy reference area (the area of energy usage) being 32,200 m^2, with reference heat demand of $2,254,000$ kWh and annual electricity consumption of 807,000 m^2. The school is equipped with a ground sourced HP of maximum power of 307 kW, 437 kW PV array, combined battery capacity of 1441 and no discrete thermal storage (thermal storage water tanks). Whereas the office is much smaller in area of approximately 600 m^2. The office is equipped with 80 kWh battery and 30 kW PV array and a ground sourced HP without domestic hot water storage. The numerical experiment includes addition of thermal reservoirs, reduction of battery and solar capacity and comparison of the outcomes with measured data. The addition of thermal reservoirs is aimed to reduce initial investments since thermal storage is significantly cheaper than electrochemical counterparts [36] and would allow the reduction of battery capacity. Thus, 2000 kWh and 100 kWh, thermal storage reservoirs (thermal storage water tanks) for space heating were added to the school and to the office respectively for the performance comparison. There is also additional analysis for implementation of RED WoLF algorithm just to control the battery and allow power flow to the heating system. Moreover, the addition of thermal storage to HP might slightly increase energy consumption of the system [69], however this effect is negligible whenever the temperature of storage is set for 45 – 55 C°. Nevertheless, the assumption the overall daily consumption for space heating and domestic hot water is increased by 5 % in case thermal storage was added to the system. This value is much higher than ≈ 1% noticed by Arteconi et al. [69], however such increase allows to reduce the chance of overestimation of monthly and annual systems performance. In addition to that standard RED WoLF configuration [35] with SH and domestic hot water cylinder is compared with measured consumption. Since in both system space heating is based on usage of the resistor rather than thermal machine, the daily consumption for space heating is assumed to be 4 times of the measured. Slightly higher than the medium COP of HP of 3.6, [70].

On Table 1 it is demonstrated that the system equipped with SH have comparable performance to the system equipped with a HP, without storage reservoirs. In case of the school emissions with RED WoLF HSS equipped with SH are slightly higher. However, in case of the office opposite statement is valid. In all cases the RED WoLF HSS with SHs, performs worse than a system equipped with HP and Thermal Storage Water Tanks. As a result, the RED WoLF HSS could become an alternative to HP, where restrictions or implementation makes it difficult to install the latter.

The RED WoLF with SH could be a financially beneficial option for smaller facilities, since HP require significant initial investments and potential major building redesign [36]. Currently the average price per peak power for PV array is ≈ 2,000 GBP per peak kW. Thus making the price of 437 kW peak PV array to be ≈ 874,000 GBP. Moreover, the average price of the ground source HPs installation could vary from ≈ 17,000 GBP for 4 kW peak power to ≈ 35,000 GBP for 13 kW peak power. Leading, to 307 kW peak power ground sourced HP cost of ≈ 826,537 GBP. In the worst-case scenario storage heaters or thermal store consume on average 4 times more electrical energy than a HP. As a result, more expensive of the shelf SHs such as Quantum Dimplex with output power of 1.5 kW would cost ≈ 623,055 GBP, whereas medium priced Elnur SHs with the same output would cost ≈ 508,109, with some of the cheapest manual models having price as low as ≈ 163,000 GBP. All these models are supported by the RED WoLF controller. Furthermore, reducing the size by of the PV array in half by the means of the RED WoLF controller would save ≈ 437,000 GBP. As a result financial savings from the system implementation are expected to be at least of ≈ 1,000,000 GBP. Moreover, the addition of a thermal storage to ground sourced HP might vary in price from ≈ 30,000 GBP to ≈ 160,000 GBP, depending on if the storage unit is single or there are many units of smaller size. This leads to RED WoLF controller allowing more moderate savings of ≈ 277,000 GBP.

Now, since each SH could act independently they have potential to satisfy different space heating requirements throughout facilities. Thus, creating with ease different thermal areas within one facility that could be useful for comfort or industrial processes. Results of the analysis are very promising; however the lack of widespread availability of time-of-use or dynamic tariffs such as [7], reduces the financial benefits of the RED WoLF system. Nevertheless, such energy tariffs emerge in more and more regions including NWE.

The results of numerical experiment are discussed below. Fig. 6 demonstrates that system with RED WoLF controller is beneficial and have potential to reduce CO_2 emissions even for systems equipped with reduced PV array. Moreover, separation of storage reservoirs is slightly more beneficial, than system equipped only with battery. Additionally, the RED WoLF controller has the ability to reduce the grid consumption as depicted in Fig. 1. However, this effect is more moderate with comparison to CO_2 emissions reduction. Furthermore, reducing the size of the PV by half slightly increases the overall consumption from the Grid. Intriguingly, monthly emissions as depicted on Fig. 8, although in general follow the pattern of annual emissions in some months. March, April, September and October the system equipped with smaller PV array produces more emissions. Though, systems with smaller PV array have significantly less emissions during winter months. This phenomenon could be due to lower overall PV power generation during winter months and increased consumption and thus storage control has more prominent effect, than local power generation. Moreover, in warmer month there is less demand for heating and generated renewable power cover the consumption requirements even with smaller PV array. Whereas, in intermediate periods there is lack of local generated power that storage of grid electricity during time intervals of lowest CO_2 index control does not fully compensate. RED WoLF with thermal storage was estimated to consume less grid electricity than original measured consumption. The same hold in general true for the system equipped with the battery storage only, however in some months the consumption could be higher. As expected with lower PV array there is more grid consumption in all months. Overall even the RED WoLF is not aimed to improving self-consumption of the facility it does it implicitly while reducing the CO_2 emissions (see Fig. 7).

Annual grid consumption (Fig. 11) and CO_2 emissions (Fig. 10) from the school have similar structure to one noticed in office. The

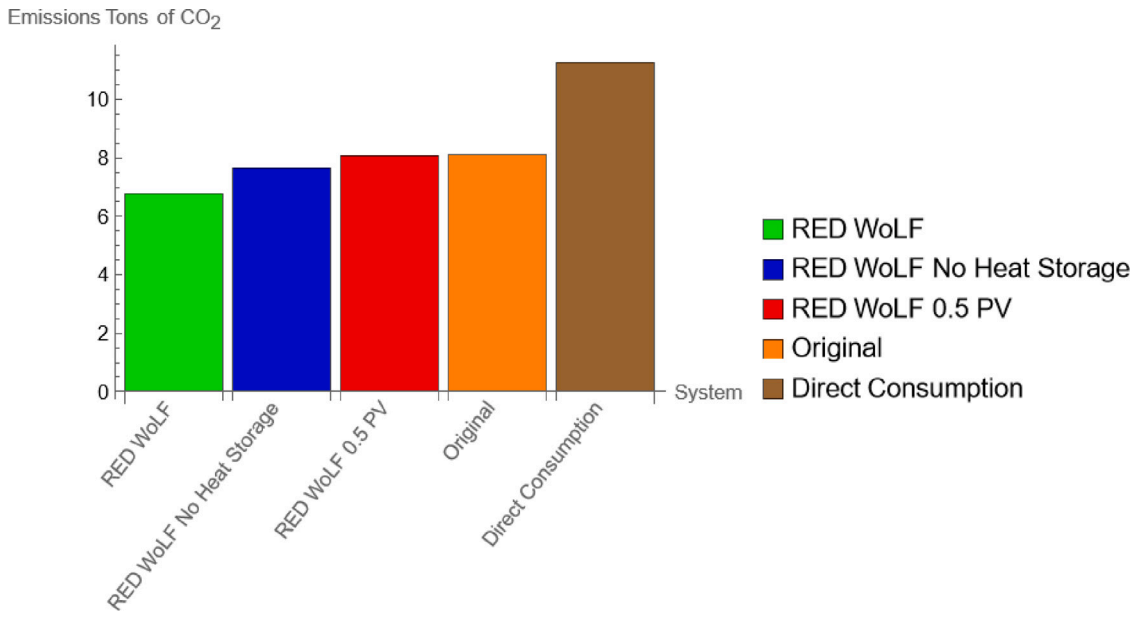

Fig. 6. Annual Emissions of CO_2 in the Office. The brown box corresponds to CO_2 emissions in the absence of PV array. The orange box corresponds to measured CO_2 emissions. The red box corresponds to estimated CO_2 emissions with RED WoLF system with PV array being 0.5 size of the original one. The blue box corresponds to estimated CO_2 emissions with RED WoLF system in the absence of heat storage. The green box corresponds to estimated CO_2 emissions with full RED WoLF system. (For interpretation of the references to colour in this figure legend, the reader is referred to the web version of this article.)

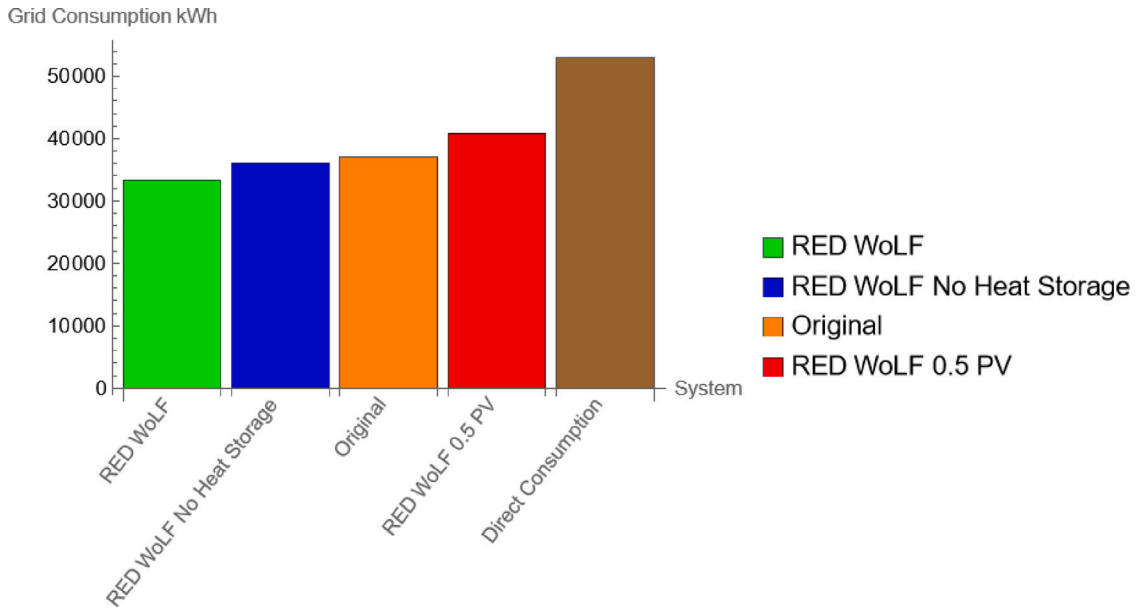

Fig. 7. Annual grid consumption in the Office. The brown box correspond to the grid consumption in the absence of PV array. The orange box correspond to measured grid consumption. The red box correspond to the estimated grid consumption with RED WoLF system with PV array being 0.5 size of the original one. The blue box correspond to the estimated grid consumption with RED WoLF system in the absence of heat storage. The green box correspond to the estimated grid consumption with full RED WoLF system. (For interpretation of the references to colour in this figure legend, the reader is referred to the web version of this article.)

reduction of the PV array and implementation of the RED WoLF algorithm reduces CO_2 emissions. However, it also increases the power intake from the Grid. Furthermore, doubling the size of the thermal storage may lead to improving reduction of CO_2, with comparison to the double increase of the battery capacity. Nevertheless: the statement is opposite for power consumption, the system with double thermal storage consume more energy than system with doubled battery storage (see Fig. 9).

Monthly CO_2 emissions in the school are depicted on Fig. 12. It could be observed, that the system without PV array and energy storage have the most emissions. Furthermore, systems with the original size of PV array have no CO_2 emissions during summer months. The proposed RED WoLF system have produced no emissions also in May. Nevertheless, from, February till October the system with half sized PV array emits more CO_2 than the original system. Though, in the remaining months such configuration performs better. As expected the proposed RED WoLF configuration equipped with thermal storage water cylinder performs better in all months, with second best system being the one with only battery storage controlled by the RED WoLF algorithm, with exception to two months: January and December.

Similarly monthly grid consumption in the school is presented on Fig. 12. Likewise, systems equipped with original PV array and in the presence of storage, have not consumed grid electricity during Summer months. Moreover, the RED WoLF system also have not consumed

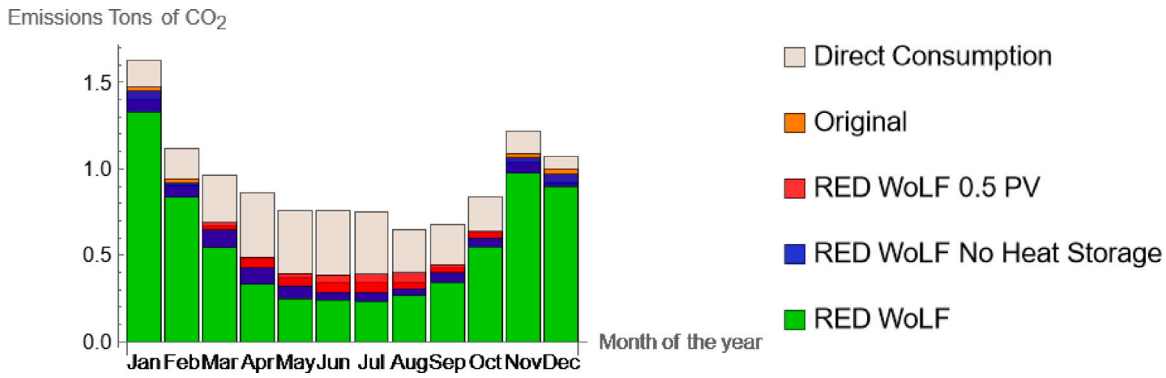

Fig. 8. Monthly Emissions of CO_2 in Office. The cream box corresponds to CO_2 emissions in the absence of PV array. The orange box corresponds to measured CO_2 emissions. The red box corresponds to estimated CO_2 emissions with RED WoLF system with PV array being 0.5 size of the original one. The blue box corresponds to estimated CO_2 emissions with RED WoLF system in the absence of heat storage. The green box corresponds to estimated CO_2 emissions with full RED WoLF system. (For interpretation of the references to colour in this figure legend, the reader is referred to the web version of this article.)

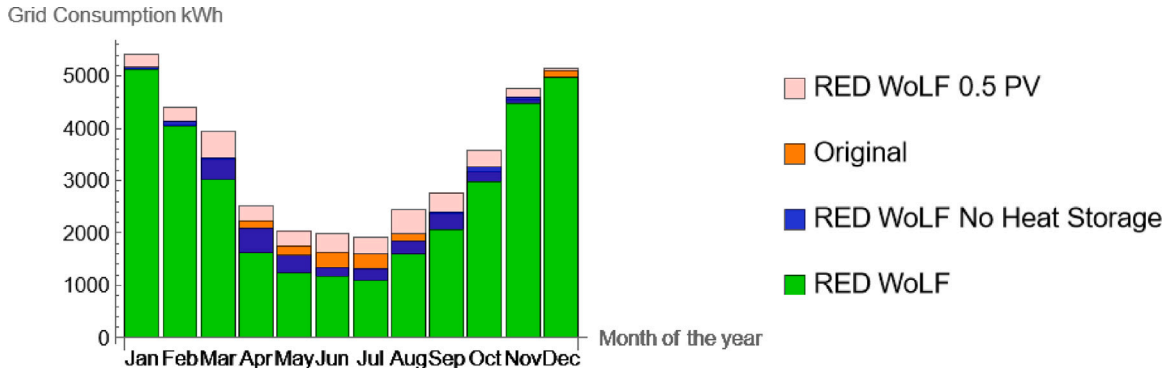

Fig. 9. Monthly grid consumption in the Office. The orange box corresponds to measured grid consumption. The cream box corresponds to the estimated grid consumption with RED WoLF system with PV array being 0.5 size of the original one. The blue box corresponds to the estimated grid consumption with RED WoLF system in the absence of heat storage. The green box corresponds to the estimated grid consumption with full RED WoLF system. (For interpretation of the references to colour in this figure legend, the reader is referred to the web version of this article.)

any power from the Grid in May. Yet, with exception to January and December less grid electricity is consumed by with RED WoLF HSS. Furthermore, in case there is no thermal storage and RED WoLF control is present the previous statement holds true also in November. As expected of all systems with RED WoLF control strategy the system with half sized PV array consume more electricity from the Grid in all months, due to lack of local renewable power generation.

Overall, the application of the RED WoLF algorithm in both cases of the school and the office reduces both CO_2 emissions and consumption annually. Moreover, the addition of the RED WoLF controller have also potential to produce lower CO_2 emissions for systems with smaller PV arrays, thus improving the self-consumption of targeted facility. As a result, less initial investment could be required to achieve similar performance and has the ability to facilitate penetration of RED WoLF HSS. The proposed RED WoLF HSS has potential to save $\approx$ 30 tonnes of CO_2 annually for the school, which is $\approx$ 22 % improvement. In case of the office the RED WoLF HSS has potential to $\approx$ 1.3 tonnes of CO_2, that corresponds to $\approx$ 16 % improvement. Less prominent reduction is noticed in case of the annual grid consumption $\approx$ 39,520 kWh, $\approx$ 6.5 % for the school and $\approx$ 3586 kWh, $\approx$ 10 % for the office. Furthermore, the RED WoLF control architecture have potential to improve off-grid performance (see Fig. 13).

4. Conclusion

The progressive adaptive double threshold approach has been improved to recursive progressive adaptive multi threshold approach. Heat pumps connected with thermal storage (thermal storage water tank, thermal storage radiators, combination of previous ones with storage heaters) or with battery are now supported by the RED WoLF controller. The newest control strategy outperformed the original RED WoLF single threshold approach by improving the reduction of CO_2 emissions by $\approx$ 26% and $\approx$ 9% to RED WoLF progressive adaptive double threshold approach. Though, underperformed with comparison to Primal Dual Simplex Method by $\approx$ 4%. Despite that, since the root mean square percentage error for CO_2 is at least $\approx$ 7.5%, could be as high as $\approx$ 73% and aggregate errors of forecast signals would be even higher, making approaches with higher accuracy not required for CO_2 reduction purposes. Although this phenomena could be more relevant for cases where predictions become more accurate. However, the speed of calculation for the RED WoLF algorithm is at least 100 times faster, making the RED WoLF controller suitable for embedded systems or to increase the resolution of control system possible. Moreover, the controller also allows slight reduction of charge/discharge cycles annually for battery storage $\approx$ 394 cycles for system equipped with primal dual simplex method, $\approx$ 329 cycles for systems equipped with RED WoLF recursive progressive adaptive multi threshold approach and $\approx$ 238 cycles for system equipped with RED WoLF progressive adaptive single threshold approach. Furthermore. all these methods have significant reduction in storage cycles with comparison to Olivieri and McConky controller in accordance to previous comparison of the latter with RED WoLF single threshold approach.

Results of numerical experiment suggest that the system equipped with RED WoLF controller outperforms both in reducing CO_2 emissions and electrical grid consumption of the system equipped with heat pump, photovoltaic array and battery with on default (non RED WoLF) logic control for the school and the office in Luxembourg. On default control has no sophisticated logic and battery is charged by

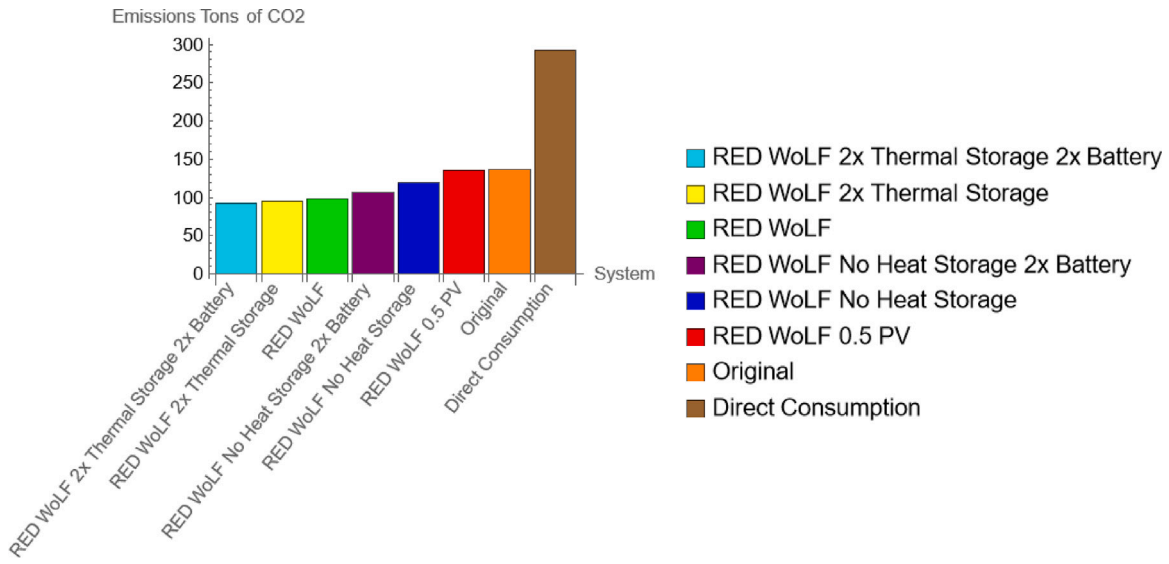

Fig. 10. Annual Emissions of CO_2 in the School. The brown box corresponds to CO_2 emissions in the absence of PV array. The orange box corresponds to measured CO_2 emissions. The red box corresponds to estimated CO_2 emissions with RED WoLF system with PV array being 0.5 size of the original one. The blue box corresponds to estimated CO_2 emissions with RED WoLF system in the absence of heat storage. The purple box corresponds to estimated CO_2 emissions with RED WoLF system in the absence of heat storage however with doubled battery capacity. The green box corresponds to estimated CO_2 emissions with full RED WoLF system. The yellow box corresponds to estimated CO_2 emissions with full RED WoLF system and doubled thermal storage. The cyan box corresponds to estimated CO_2 emissions with full RED WoLF system and doubled thermal storage and doubled battery capacity. (For interpretation of the references to colour in this figure legend, the reader is referred to the web version of this article.)

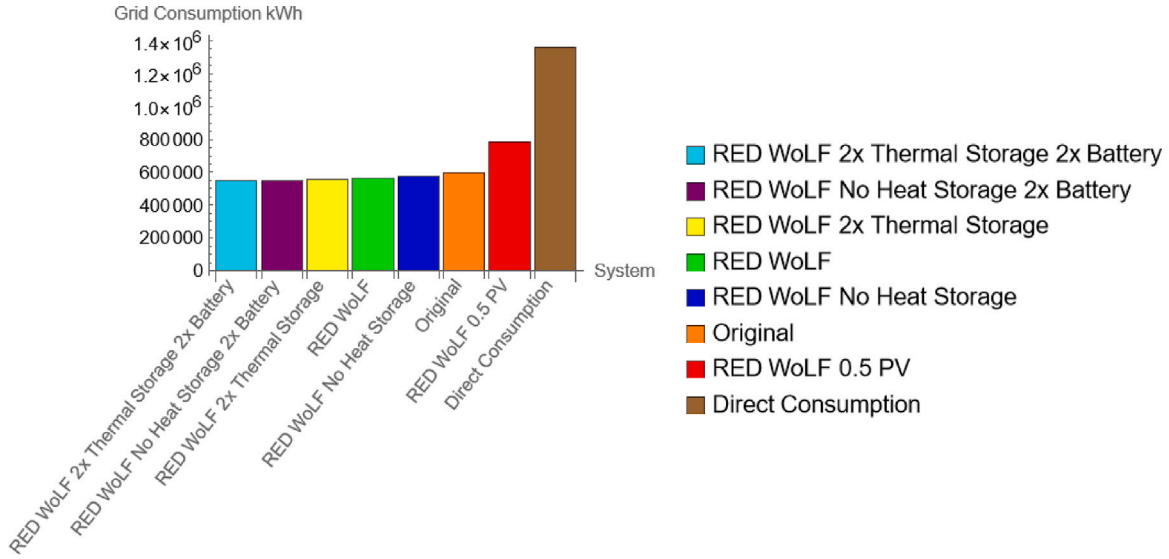

Fig. 11. Annual grid consumption in the School. The brown box corresponds to the grid consumption in the absence of PV array. The orange box corresponds to measured grid consumption emissions. The red box corresponds to estimated grid consumption emissions with RED WoLF system with PV array being 0.5 size of the original one. The blue box corresponds to estimated grid consumption with RED WoLF system in the absence of heat storage. The purple box corresponds to estimated grid consumption with RED WoLF system in the absence of heat storage however with doubled battery capacity. The green box corresponds to estimated grid consumption with full RED WoLF system. The yellow box corresponds to estimated grid consumption with full RED WoLF system and doubled thermal storage. The cyan box corresponds to estimated grid consumption with full RED WoLF system and doubled thermal storage and doubled battery capacity. (For interpretation of the references to colour in this figure legend, the reader is referred to the web version of this article.)

photovoltaic array by excess of generated power. Such performance is quite good, as most of consumption in facilities, that operate in average 9 – 5 working hours, occurs during the time whenever photovoltaic power is also generated. Furthermore, the reduction of CO_2 emissions is more prominent than electricity intake from the grid. Additional elements such as thermal storage could further improve the performance. Even decreasing photovoltaic array by half still have better estimated performance than system without control, thus allowing to reduce significantly the overall initial investment to the energy management system. Intriguingly, the system equipped with storage heaters, have potential to reduce more CO_2 emissions than systems with heat pump in absence of photovoltaic array and battery storage, despite storage heaters consuming at least 3.6 more power, that further could amplify reduction of initial investments. In the office CO_2 emissions with RED WoLF controller and SHs as heating system are $\approx$ 9.7 tonnes, are $\approx$ 11.3 tonnes for direct heat pump consumption and are $\approx$ 8.1 tonnes for system with default control strategy. Making system equipped with storage heater a cheaper alternative to systems equipped with heat pumps, where the installation of latter is not cost-effective solution. Nevertheless, the example of the school system equipped with heat pump leads to $\approx$ 2.5 times more CO_2 emission savings than system with storage heaters. Thus, additional assessment is required to analyse cost

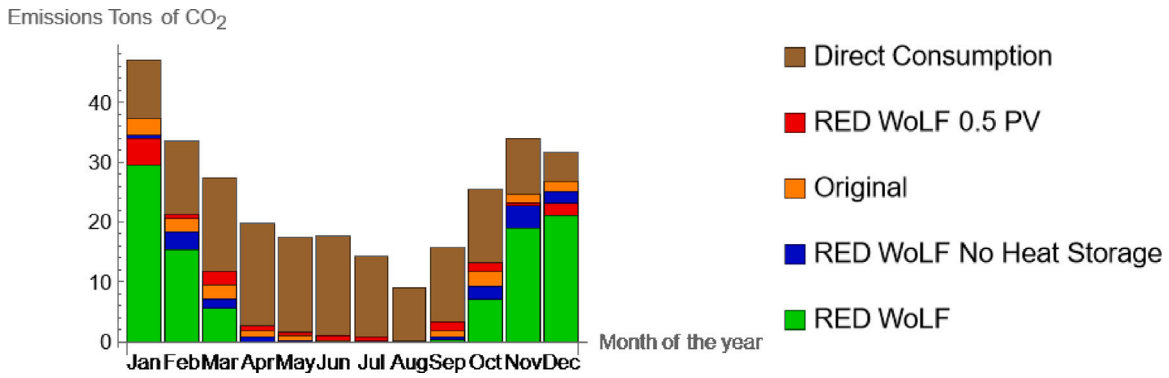

Fig. 12. Monthly Emissions of CO_2 in the School. The brown box corresponds to CO_2 emissions in the absence of PV array. The orange box corresponds to measured CO_2 emissions. The red box corresponds to estimated CO_2 emissions with RED WoLF system with PV array being 0.5 size of the original one. The blue box corresponds to estimated CO_2 emissions with RED WoLF system in the absence of heat storage. The green box corresponds to estimated CO_2 emissions with full RED WoLF system. (For interpretation of the references to colour in this figure legend, the reader is referred to the web version of this article.)

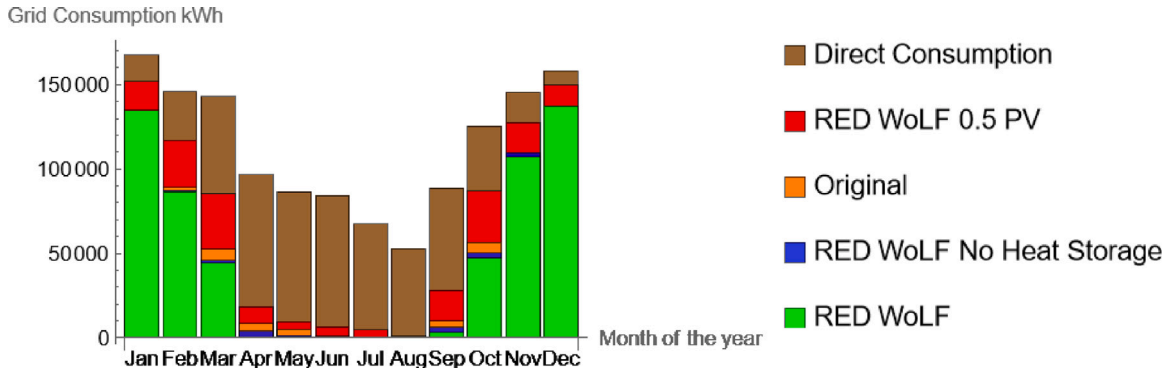

Fig. 13. Monthly grid consumption in the School. The brown box corresponds to the grid consumption in the absence of PV array. The orange box corresponds to measured grid consumption emissions. The red box corresponds to estimated grid consumption emissions with RED WoLF system with PV array being 0.5 size of the original one. The blue box corresponds to estimated grid consumption with RED WoLF system in the absence of heat storage. The green box corresponds to estimated grid consumption with full RED WoLF system. (For interpretation of the references to colour in this figure legend, the reader is referred to the web version of this article.)

benefits to comprehend which selection is better for each particular case.

As a result, the RED WoLF controller has ability to be implemented both in residential, public facilities, offices and commercial facilities. The speed of the RED WoLF computation allows the algorithm to be implemented on edge systems or to control multiple systems with server, for example the RED WoLF controller is able to govern energy management systems in 100 pilot houses with medium performance RAC server. The performance in CO_2 reduction is comparable with primal dual simplex optimisation. The adaptable mechanism applied in the system allows the storage targets to be changed during control implementation on intraday basis, as well as the system is designed to guarantee that all storage targets will be met, even if the performance is suboptimal, that is important for employment in multiple disjoint facilities, where underperformance is not acceptable, such as social houses. Making the RED WoLF simulation environment having potential application in fast assessment of environmental, financial performance of energy management systems. Furthermore, successful implementation of RED WoLF Controller in educational programmes benefit students to understand grid related carbon emissions as well as introduce to energy management systems, without necessity of any prior field specific knowledge.

Declaration of competing interest

The authors declare that they have no known competing financial interests or personal relationships that could have appeared to influence the work reported in this paper.

Data availability

Data will be made available on request.

Acknowledgements

This work has been supported by the European Regional Development Fund, project RED WoLF, project number NWE847

Appendix. Threshold calculation

The main mathematical formulation behind the double-threshold approach described in [36] is presented here in order to facilitate comprehension of Section 2.1.

There are constantly changing variables (Table A.2) associated with dynamic environment as well as static parameters associated with physical properties of energy storage reservoirs (Table A.3) crucial to thresholds calculation. The algorithm is deciding whether to charge or idle thermal storage and whether to charge, discharge or idle electrochemical storage in the form of a battery. The decision to charge energy storage reservoirs from the grid is made if the target signal is below the main threshold. The decision to discharge battery is made if the target signal is above the auxiliary threshold. Moreover, the battery stops charging from the grid if there is no more predicted power intake to appliances in the next 24 h. These predictions are then updated every hour. In summary thresholds are designed to calculated the minimum averaged amount of time required for the system to fully charge storage reservoirs from the electrical grid and to use battery storage during hours with high CO_2 emissions.

Table A.2
List of variables.

B_D	Battery demand in kW.
B_{Level}	Battery level in kWh.
C_D	Water Cylinder Demand.
C_{Level}	Water Cylinder Level in kWh.
C_{Setup}	Water Cylinder Level Storage Target in kWh.
$\tilde{H}_D$	Space Heating Demand in kW.
$\tilde{H}_{Level}$	Space Heating Level in kWh.
$\tilde{H}_{Setup}$	Space Heating Level Storage Target in kWh.
P_{P2A}	Predicted Power Consumption by Appliances in kW.
P_{PV}	Predicted Power Generation by PV Array in kW.
Q	CO_2 intensity level prediction in gCO_2/kWh.
δ	Main threshold in gCO_2/kWh.
δ_{aux}	Auxiliary threshold in gCO_2/kWh.

Table A.3
List of parameters.

B_{Max}	Maximum Rate of Power intake by a Battery in kW.
B_{LMax}	Maximum Capacity of a Battery in kWh.
C_Max	Maximum Rate of Power intake of a Water Cylinder in kW.
C_{LMax}	Maximum Energy Storage Level of a Water Cylinder in kWh.
$\tilde{H}_{Max}$	Maximum Rate of Power intake of a Space Heating System in kW.
$\tilde{H}_{LMax}$	Maximum Energy Storage Level of a Space Heating System in kW.

In order to calculate the main threshold first the demand for energy storage is established

$$B_D = B_{Max} H(B_{Setup} - B_{Level}) H(B_{LMax} - B_{Level}),$$
$$C_D = C_{Max} H(C_{Setup} - C_{Level}) H(C_{LMax} - C_{Level}),$$
$$\tilde{H}_D = \tilde{H}_{Max} H(\tilde{H}_{Setup} - \tilde{H}_{Level}) H(\tilde{H}_{LMax} - \tilde{H}_{Level}),$$

where $H(x)$ is a Heaviside step function, the demand function have starting value in the domain being 0 and end value being $\mathcal{T}$. Here $\mathcal{T}$ is a horizon period of the algorithm execution. Then the integral balance of the system for the selected period of $\mathcal{T}$ hours is defined as

$$\mathcal{I} = \int_{\hat{t}}^{\mathcal{T}} P_{P2A}(t) - P_{PV}(t) dt + C_{Setup} - C_{Level} + \tilde{H}_{Setup} - \tilde{H}_{Level}, \tag{A.1}$$

where $\hat{t}$ is the current execution time within $\mathcal{T}$ hours period. If $\tilde{H}_{LMax} \tilde{H}_{Setup}$ or $C_{LMax} < C_{Setup}$ then $\tilde{H}_{Setup}$ and C_{Setup} are substituted by $\tilde{H}_{LMax}$ and C_{LMax} in Eq. (A.1) respectively. Moreover, if in any moment during $\mathcal{T}$ period $C_{Setup} = C_{Level}$ or $\tilde{H}_{Setup} = \tilde{H}_{Level}$ then variables with C or $\tilde{H}$ are dropped from Eq. (A.1) respectively. That is slightly different to [36] as $\tilde{H}$ is also involved in computations. Such procedure allow to prevent storage being overcharged from the grid. The excess power from the PV array not required for the appliances consumption is still allowed to be directed to the energy storage. Then the rate of power intake is introduced as

$$\omega = \frac{\int_{\hat{t}}^{\mathcal{T}} P_{P2A}(t) dt}{\mathcal{T} - \hat{t}} + B_{Max} + C_{Max} + \tilde{H}_{Max}.$$

Knowing the rate of power intake and integral balance allows the calculation of averaged minimum amount of time required for system to be charged from the electrical grid, yielding

$$I > 0 \wedge \mathcal{T}_{Int} = \max\left(\frac{60I}{\omega}, \frac{C_{Setup} - C_{Level}}{C_{Max}}, \frac{\tilde{H}_{Setup} - \tilde{H}_{Level}}{\tilde{H}_{Max}}\right),$$
$$I \leq 0 \wedge \mathcal{T}_{Int} = 0.$$

Now the carbon intensity time series Q is sorted in monotonically increasing order as Q_{sort} allowing to define the main threshold as $\delta = Q_{sort}(\mathcal{T}_{Int})$. Here is the moment where the back coefficient is added in order to avoid on demand charging of heating system as $\delta = Q_{sort}(\mathcal{T} + b * 60)$. That is done by simulating the system operation and if in any moment on demand operation of either DHW Cylinder or Thermal Storage is expected to be turn on, more energy is allowed to be stored from the grid. This operation continues until no power on demand is predicted to be directed from the grid to thermal storage reservoirs. Calculation of δ_{aux} is in agreement with [36], though the time interval of operation is restricted to 24 h.

References

[1] COP27. Sharm el-sheikh climate change conference. 2022, URL https://unfccc.int/cop27.

[2] ECF. A practical guide to a prosperous, low-carbon Europe. 2010, https://www.roadmap2050.eu/.

[3] Kotsopoulos D. Organizational energy conservation matters in the anthropocene. Energies 2022;15(21). http://dx.doi.org/10.3390/en15218214, URL https://www.mdpi.com/1996-1073/15/21/8214.

[4] Horizon Europe. 2023, URL https://research-and-innovation.ec.europa.eu/funding/funding-opportunities/funding-programmes-and-open-calls/horizon-europe_en.

[5] Interreg North-West Eruope. Cooperation Programme Interreg North-West Europe 2021 - 2027. 2023, https://www.nweurope.eu/.

[6] Department for Business energy & Industrial Strategy. Energy Flow Chart 2021. 2021, URL https://assets.publishing.service.gov.uk/government/uploads/system/uploads/attachment_data/file/1093445/Energy_Flow_Chart_2021.pdf.

[7] Ocotpus Energy. Octopus energy agile. 2020, URL octopus.energy.

[8] Carbon Intensity. Carbon intensity API. 2020, URL https://carbonintensity.org.uk/.

[9] Electricity Maps. 2023, URL https://www.electricitymaps.com/.

[10] Zhang N, Lu X, McElroy MB, Nielsen CP, Chen X, Deng Y, et al. Reducing curtailment of wind electricity in China by employing electric boilers for heat and pumped hydro for energy storage. Appl Energy 2016;184:987–94.

[11] Andoni M, Robu V, Früh W-G, Flynn D. Game-theoretic modeling of curtailment rules and network investments with distributed generation. Appl Energy 2017;201:174–87.

[12] Le KX, Huang MJ, Wilson C, Shah NN, Hewitt NJ. Tariff-based load shifting for domestic cascade heat pump with enhanced system energy efficiency and reduced wind power curtailment. Appl Energy 2020;257:113976.

[13] Mills AD, Wiser RH. Strategies to mitigate declines in the economic value of wind and solar at high penetration in california. Appl Energy 2015;147:269–78.

[14] Hou Q, Zhang N, Du E, Miao M, Peng F, Kang C. Probabilistic duck curve in high PV penetration power system: Concept, modeling, and empirical analysis in China. Appl Energy 2019;242:205–15.

[15] Ederer N. The market value and impact of offshore wind on the electricity spot market: Evidence from Germany. Appl Energy 2015;154:805–14.

[16] Wagh M, Kulkarni V. Modeling and optimization of integration of renewable energy resources (RER) for minimum energy cost, minimum CO2 emissions and sustainable development, in recent years: A review. Mater Today: Proc 2018;5(1, Part 1):11–21. http://dx.doi.org/10.1016/j.matpr.2017.11.047, International Conference on Processing of Materials, Minerals and Energy (July 29th - 30th) 2016, Ongole, Andhra Pradesh, India.

[17] Mohamad F, Teh J, Lai C-M, Chen L-R. Development of energy storage systems for power network reliability: A review. Energies 2018;11(9). http://dx.doi.org/10.3390/en11092278, URL https://www.mdpi.com/1996-1073/11/9/2278.

[18] Mohamad F, Teh J. Impacts of energy storage system on power system reliability: A systematic review. Energies 2018;11(7). http://dx.doi.org/10.3390/en11071749, URL https://www.mdpi.com/1996-1073/11/7/1749.

[19] Grosspietsch D, Saenger M, Girod B. Matching decentralized energy production and local consumption: A review of renewable energy systems with conversion and storage technologies. WIREs Energy Environ 2019;8(4):e336. http://dx.doi.org/10.1002/wene.336, arXiv:https://onlinelibrary.wiley.com/doi/pdf/10.1002/wene.336.

[20] Luthander R, Widén J, Nilsson D, Palm J. Photovoltaic self-consumption in buildings: A review. Appl Energy 2015;142:80–94. http://dx.doi.org/10.1016/j.apenergy.2014.12.028, URL http://www.sciencedirect.com/science/article/pii/S0306261914012859.

[21] McKenna E, McManus M, Cooper S, Thomson M. Economic and environmental impact of lead-acid batteries in grid-connected domestic PV systems. Appl Energy 2013;104:239–49. http://dx.doi.org/10.1016/j.apenergy.2012.11.016, URL http://www.sciencedirect.com/science/article/pii/S0306261912008094.

[22] Widén J. Improved photovoltaic self-consumption with appliance scheduling in 200 single-family buildings. Appl Energy 2014;126:199–212. http://dx.doi.org/10.1016/j.apenergy.2014.04.008, URL http://www.sciencedirect.com/science/article/pii/S0306261914003419.

[23] Hernández J, Sanchez-Sutil F, Muñoz-Rodríguez F. Design criteria for the optimal sizing of a hybrid energy storage system in PV household-prosumers to maximize self-consumption and self-sufficiency. Energy 2019;186:115827. http://dx.doi.org/10.1016/j.energy.2019.07.157, URL https://www.sciencedirect.com/science/article/pii/S0360544219314999.

[24] Hernández J, Sanchez-Sutil F, Muñoz-Rodríguez F, Baier C. Optimal sizing and management strategy for PV household-prosumers with self-consumption/sufficiency enhancement and provision of frequency containment reserve. Appl Energy 2020;277:115529. http://dx.doi.org/10.1016/j.apenergy.2020.115529, URL https://www.sciencedirect.com/science/article/pii/S0306261920310412.

[25] Gomez-Gonzalez M, Hernandez J, Vera D, Jurado F. Optimal sizing and power schedule in PV household-prosumers for improving PV self-consumption and providing frequency containment reserve. Energy 2020;191:116554. http://dx.doi.org/10.1016/j.energy.2019.116554, URL https://www.sciencedirect.com/science/article/pii/S0360544219322492.

[26] Muñoz-Rodríguez FJ, Jiménez-Castillo G, de la Casa Hernández J, Aguilar Peña JD. A new tool to analysing photovoltaic self-consumption systems with batteries. Renew Energy 2021;168:1327–43. http://dx.doi.org/10.1016/j.renene.2020.12.060, URL https://www.sciencedirect.com/science/article/pii/S0960148120319984.

[27] Uddin M, Romlie MF, Abdullah MF, Halim SA, Bakar AHA, Kwang TC. A review on peak load shaving strategies. Renew Sustain Energy Rev 2018;82:3323–32. http://dx.doi.org/10.1016/j.rser.2017.10.056.

[28] Sufyan M, Rahim NA, Aman MM, Tan CK, Raihan SRS. Sizing and applications of battery energy storage technologies in smart grid system: A review. J Renew Sustain Energy 2019;11(1):014105.

[29] Arani AK, Gharehpetian GB, Abedi M. Review on energy storage systems control methods in microgrids. Int J Electr Power Energy Syst 2019;107:745–57. http://dx.doi.org/10.1016/j.ijepes.2018.12.040.

[30] Wu B, Widanage WD, Yang S, Liu X. Battery digital twins: Perspectives on the fusion of models, data and artificial intelligence for smart battery management systems. Energy and AI 2020;1:100016. http://dx.doi.org/10.1016/j.egyai.2020.100016, URL https://www.sciencedirect.com/science/article/pii/S2666546820300161.

[31] Yan J, Yang X. Thermal energy storage. Appl Energy 2019;240:A1 – A6. http://dx.doi.org/10.1016/j.apenergy.2018.03.001, URL http://www.sciencedirect.com/science/article/pii/S0306261918303179.

[32] Baeten B, Rogiers F, Helsen L. Reduction of heat pump induced peak electricity use and required generation capacity through thermal energy storage and demand response. Appl Energy 2017;195:184–95. http://dx.doi.org/10.1016/j.apenergy.2017.03.055, URL http://www.sciencedirect.com/science/article/pii/S0306261917302854.

[33] Felten B, Weber C. The value(s) of flexible heat pumps – assessment of technical and economic conditions. Appl Energy 2018;228:1292–319. http://dx.doi.org/10.1016/j.apenergy.2018.06.031, URL http://www.sciencedirect.com/science/article/pii/S0306261918309000.

[34] Reda F, Fatima Z. Northern European nearly zero energy building concepts for apartment buildings using integrated solar technologies and dynamic occupancy profile: Focus on Finland and other northern European countries. Appl Energy 2019;237:598–617. http://dx.doi.org/10.1016/j.apenergy.2019.01.029, URL http://www.sciencedirect.com/science/article/pii/S0306261919300297.

[35] Shukhobodskiy AA, Colantuono G. RED WoLF: Combining a battery and thermal energy reservoirs as a hybrid storage system. Appl Energy 2020;274. http://dx.doi.org/10.1016/j.apenergy.2020.115209, URL www.scopus.com.

[36] Shukhobodskiy AA, Zaitcev A, Pogarskaia T, Colantuono G. RED WoLF hybrid storage system: Comparison of CO2 and price targets. J Clean Prod 2021;321:128926. http://dx.doi.org/10.1016/j.jclepro.2021.128926, URL https://www.sciencedirect.com/science/article/pii/S0959652621030419.

[37] Telaretti E, Graditi G, Ippolito MG, Zizzo G. Economic feasibility of stationary electrochemical storages for electric bill management applications: The Italian scenario. Energy Policy 2016;94:126–37, URL www.scopus.com, Cited By :34.

[38] Zhou Y, Zheng S. Machine-learning based hybrid demand-side controller for high-rise office buildings with high energy flexibilities. Appl Energy 2020;262:114416. http://dx.doi.org/10.1016/j.apenergy.2019.114416, URL https://www.sciencedirect.com/science/article/pii/S0306261919321038.

[39] Liu C, Sun B, Zhang C, Li F. A hybrid prediction model for residential electricity consumption using holt-winters and extreme learning machine. Appl Energy 2020;275:115383. http://dx.doi.org/10.1016/j.apenergy.2020.115383, URL https://www.sciencedirect.com/science/article/pii/S0306261920308953.

[40] Yang S, Wan MP, Chen W, Ng BF, Dubey S. Model predictive control with adaptive machine-learning-based model for building energy efficiency and comfort optimization. Appl Energy 2020;271:115147. http://dx.doi.org/10.1016/j.apenergy.2020.115147, URL https://www.sciencedirect.com/science/article/pii/S0306261920306590.

[41] Shivam K, Tzou J-C, Wu S-C. A multi-objective predictive energy management strategy for residential grid-connected PV-battery hybrid systems based on machine learning technique. Energy Convers Manage 2021;237:114103. http://dx.doi.org/10.1016/j.enconman.2021.114103, URL https://www.sciencedirect.com/science/article/pii/S019689042100279X.

[42] Amini Toosi H, Del Pero C, Leonforte F, Lavagna M, Aste N. Machine learning for performance prediction in smart buildings: Photovoltaic self-consumption and life cycle cost optimization. Appl Energy 2023;334:120648. http://dx.doi.org/10.1016/j.apenergy.2023.120648, URL https://www.sciencedirect.com/science/article/pii/S0306261923000120.

[43] Yu L, Xie W, Xie D, Zou Y, Zhang D, Sun Z, et al. Deep reinforcement learning for smart home energy management. IEEE Internet Things J 2020;7(4):2751–62. http://dx.doi.org/10.1109/JIOT.2019.2957289.

[44] Mounsif M, Medard F. Smart energy management system framework for population dynamics modelling and suitable energy trajectories identification in islanded micro-grids. Energy and AI 2023;13:100242. http://dx.doi.org/10.1016/j.egyai.2023.100242, URL https://www.sciencedirect.com/science/article/pii/S2666546823000149.

[45] Kharlamova N, Hashemi S, Træholt C. Data-driven approaches for cyber defense of battery energy storage systems. Energy and AI 2021;5:100095. http://dx.doi.org/10.1016/j.egyai.2021.100095, URL https://www.sciencedirect.com/science/article/pii/S2666546821000495.

[46] Zhou Y. Artificial intelligence in renewable systems for transformation towards intelligent buildings. Energy and AI 2022;10:100182. http://dx.doi.org/10.1016/j.egyai.2022.100182, URL https://www.sciencedirect.com/science/article/pii/S2666546822000313.

[47] Xiong R, Li H, Yu Q, Romagnoli A, Jurasz J, Yang X-G. Applications of AI in advanced energy storage technologies. Energy and AI 2023;100268. http://dx.doi.org/10.1016/j.egyai.2023.100268, URL https://www.sciencedirect.com/science/article/pii/S266654682300040X.

[48] Teh J, Lai C-M. Reliability impacts of the dynamic thermal rating and battery energy storage systems on wind-integrated power networks. Sustain Energy Grids Netw 2019;20:100268. http://dx.doi.org/10.1016/j.segan.2019.100268, URL https://www.sciencedirect.com/science/article/pii/S2352467719304680.

[49] Metwaly MK, Teh J. Probabilistic peak demand matching by battery energy storage alongside dynamic thermal ratings and demand response for enhanced network reliability. IEEE Access 2020;8:181547–59. http://dx.doi.org/10.1109/ACCESS.2020.3024846.

[50] Zotov E, Kadirkamanathan V. CycleStyleGAN-based knowledge transfer for a machining digital twin. Front Artif Intell 2021;4. http://dx.doi.org/10.3389/frai.2021.767451.

[51] Boretti A. Integration of solar thermal and photovoltaic, wind, and battery energy storage through AI in NEOM city. Energy and AI 2021;3:100038. http://dx.doi.org/10.1016/j.egyai.2020.100038, URL https://www.sciencedirect.com/science/article/pii/S2666546820300380.

[52] Ortiz P, Kubler S, Rondeau É, McConky K, Shukhobodskiy AA, Colantuono G, et al. Greenhouse gas emission reduction in residential buildings: A lightweight model to be deployed on edge devices. J Clean Prod 2022;368:133092. http://dx.doi.org/10.1016/j.jclepro.2022.133092, URL https://www.sciencedirect.com/science/article/pii/S0959652622026816.

[53] Ortiz P, Kubler S, Rondeau É. CANO: A lightweight carbon emission and inhabitants' energy needs optimisation model. IFAC-PapersOnLine 2022;55(8):106–11. http://dx.doi.org/10.1016/j.ifacol.2022.08.018, URL https://www.sciencedirect.com/science/article/pii/S2405896322010916, 6th IFAC Symposium on Telematics Applications TA 2022.

[54] Pogarskaia T, Lupuleac S, Heiliö M. ECMI modelling week: First time in Russia and first time online. In: Ehrhardt M, Günther M, editors. Progress in industrial mathematics at ECMI 2021. Cham: Springer International Publishing; 2022, p. 9–15.

[55] Curet ND. A primal-dual simplex method for linear programs. Oper Res Lett 1993;13(4):233–7. http://dx.doi.org/10.1016/0167-6377(93)90045-I, URL https://www.sciencedirect.com/science/article/pii/016763779390045I.

[56] Wiesheu M, Rutešić L, Shukhobodskiy AA, Pogarskaia T, Zaitcev A, Colantuono G. RED WoLF hybrid storage system: Adaptation of algorithm and analysis of performance in residential dwellings. Renew Energy 2021;179:1036–48. http://dx.doi.org/10.1016/j.renene.2021.07.032, URL https://www.sciencedirect.com/science/article/pii/S0960148121010375.

[57] Ortiz P, Kubler S, Rondeau É, Georges J-P, Colantuono G, Shukhobodskiy AA. Greenhouse gas emission reduction system in photovoltaic nanogrid with battery and thermal storage reservoirs. J Clean Prod 2021;310:127347. http://dx.doi.org/10.1016/j.jclepro.2021.127347, URL https://www.sciencedirect.com/science/article/pii/S0959652621015663.

[58] Faticon. Faticon.com. 2023, https://www.flaticon.com/.

[59] RED WoLF - Rethink Electricity Distribution Wihout Load Following.

[60] Lau ET, Chai KK, Chen Y, Loo J. Efficient economic and resilience-based optimization for disaster recovery management of critical infrastructures. Energies 2018;11(12). http://dx.doi.org/10.3390/en11123418, URL https://www.mdpi.com/1996-1073/11/12/3418.

[61] Nasedal J, Wright S. Numerical optimization. Springer, New York; 2006.

[62] Oxford PVarray. 2016, https://shkspr.mobi/blog/2014/12/a-year-of-solar-panels-open-data/.

[63] Lichman M. UCI machine learning repository. 2013, http://archive.ics.uci.edu/ml.

[64] Colantuono G, Kor A-L, Pattinson C, Gorse C. PV with multiple storage as function of geolocation. Solar Energy 2018;165:217–32. http://dx.doi.org/10.1016/j.solener.2018.03.020.

[65] Enerdata. Enerdata intelligence + Consulting. 2019, https://www.odyssee-mure.eu/publications/efficiency-by-sector/households/electricity-consumption-dwelling.html.

[66] Olivieri ZT, McConky K. Optimization of residential battery energy storage system scheduling for cost and emissions reductions. Energy Build 2020;210:109787. http://dx.doi.org/10.1016/j.enbuild.2020.109787, URL https://www.sciencedirect.com/science/article/pii/S0378778819312150.
[67] ECO:NOVIS. Bureau d'études - ingénieurs-conseils. 2022.
[68] Energipark. Energipark réiden s.a.. 2022, https://energiepark.lu/.
[69] Arteconi A, Hewitt N, Polonara F. Domestic demand-side management (DSM): Role of heat pumps and thermal energy storage (TES) systems. Appl Therm Eng 2013;51(1):155–65. http://dx.doi.org/10.1016/j.applthermaleng.2012.09.023, URL https://www.sciencedirect.com/science/article/pii/S1359431112006357.
[70] Spitler JD, Gehlin S. Measured performance of a mixed-use commercial-building ground source heat pump system in Sweden. Energies 2019;12(10). http://dx.doi.org/10.3390/en12102020, URL https://www.mdpi.com/1996-1073/12/10/2020.